J|A|C|S
ARTICLES
Published on Web 04/06/2007

Functional Molecules from Single Wall Carbon Nanotubes. Photoinduced Solubility of Short Single Wall Carbon Nanotube Residues by Covalent Anchoring of 2,4,6-Triarylpyrylium Units

Mercedes Alvaro, Carmela Aprile, Belen Ferrer, and Hermenegildo Garcia*

Contribution from the Instituto de Tecnología Química and Departamento de Química, Universidad Politécnica de Valencia, Av. de los Naranjos s/n, 46022 Valencia, Spain

Received December 18, 2006; E-mail: hgarcia@qim.upv.es

Abstract: Raw, micrometric HiPCO single wall carbon nanotube (SWNT) material was submitted to harsh acid oxidative treatment with a 3:1 H_2SO_4/HNO_3 mixture to give short residues of SWNT (s-SWNT, <200 nm length measured by TEM). s-SWNT was functionalized through the tip carboxylic groups by peptide bonds using 3-mercatopropanamine linkers that subsequently were reacted with 2,6-diphenyl-4-(4-vinylbiphenyl)pyrylium using azobis(isobutyronitrile) as a radical initiator. After purification by dialysis, the resulting s-SWNT having covalently linked through an ethylthiopropylamide tether the strong electron-transfer pyrylium photosensitizer (Py-sSWNT) was characterized by solution ^{1}H NMR spectroscopy (observation of specific signals due to the heterocyclic protons). Emission spectroscopy shows that the fluorescence of 2,6-diphenyl-4-(4-dodecylthiobiphenyl)pyrylium (Py-SC_{12}) tetrafluoroborate (a model compound to the tethered pyrylium moiety in Py-sSWNT) (λ_{em} 533 nm) is quenched by s-SWNT and *vice versa* that the emission of s-SWNT (λ_{em} 330 nm) is quenched by Py-SC_{12}. Depending on the excitation wavelength, Py-sSWNT exhibits dual emission corresponding to each of the two moieties, but with much less intensity than each of the model components independently. Laser flash photolysis of model Py-SC_{12} allows detection of the triplet (λ_{T-T} 750 nm, τ 11.7 μs) and the much longer-lived pyrylium centered radical (λ_{max} 525 nm, τ 147 μs). The latter species arises from photoinduced electron transfer from the sulfur atom, as the donor, to the pyrylium heterocycle in its electronic excited-state, as the electron acceptor. Laser flash photolysis (355 nm) of Py-sSWNT also allows detection of the pyrylium centered radical together with a broad absorption spanning from 200 to 500 nm and peaking at 280 nm. The latter band is absent in the laser flash photolysis of the model s-SWNT and was attributed to the electron hole localized on the nanotube moiety of Py-SWNT. The most remarkable effect of the steady-state irradiation is a 1 order of magnitude increase in the solubility of Py-sSWNT. According to TEM images this photoinduced solubility can be attributed to the debundling of the nanotubes due to photoinduced charge separation through the nanotube walls. In addition to exemplify how molecular compounds with photoresponsive properties can be derived from SWNT materials, the observation of photoinduced solubility can serve to develop SWNT layers suitable for photolithography patterning.

Introduction

Single wall carbon nanotubes (SWNTs) offer promising opportunities for the development of novel materials with applications as transparent conducting electrodes,[1−4] for the construction of field-effect transistors in microelectronics,[5−8] and as components in optoelectronic materials[9,10] including organic solar cells.[1,11−13] Covalent functionalization of SWNTs attaches suitable organic moieties able to produce a response on the SWNT as a consequence of external stimuli, thus, rendering novel advanced responsive functional materials.[14−16]

(1) Du Pasquier, A.; Unalan, H. E.; Kanwal, A.; Miller, S.; Chhowalla, M. *Appl. Phys. Lett.* **2005**, *87*, 203511−203513.
(2) Kukovecz, A.; Konya, Z.; Kiricsi, I. *Encycl. Nanosci. Nanotechnol.* **2004**, *9*, 923−946.
(3) Rao, C. N. R.; Satishkumar, B. C.; Govindaraj, A.; Nath, M. *Chem. Phys. Chem.* **2001**, *2*, 78−105.
(4) Subramoney, S. *Adv. Mater.* **1998**, *10*, 1157−1171.
(5) Seidel, R.; Graham, A. P.; Unger, E.; Duesberg, G. S.; Liebau, M.; Steinhoegl, W.; Pamler, W.; Kreupl, F. *IEEE-NANO 2004, Muenchen, Germany, Aug. 16−19, 2004* **2004**, 1−3.
(6) Qi, P.; Javey, A.; Rolandi, M.; Wang, Q.; Yenilmez, E.; Dai, H. *J. Am. Chem. Soc.* **2004**, *126*, 11774−11775.
(7) Hoenlein, W.; Kreupl, F.; Duesberg, G. S.; Graham, A. P.; Liebau, M.; Seidel, R. V.; Unger, E. *IEEE Trans. Compon. Packag. Technol.* **2004**, *27*, 629−634.
(8) Hoenlein, W.; Kreupl, F.; Duesberg, G. S.; Graham, A. P.; Liebau, M.; Seidel, R.; Unger, E. *Mater. Sci. Eng., C* **2003**, *23*, 663−669.
(9) Min, Y.-S.; Bae, E. J.; Kim, U. J.; Park, W.; Hwang, C. S. *Appl. Phys. Lett.* **2006**, *89*, 113116/113111−113116/113113.
(10) Avouris, P.; Appenzeller, J. *Ind. Phys.* **2004**, *10*, 18−21.
(11) Rowell, M. W.; Topinka, M. A.; McGehee, M. D.; Prall, H.-J.; Dennler, G.; Sariciftci, N. S.; Hu, L.; Gruner, G. *Appl. Phys. Lett.* **2006**, *88*, 233506/233501−233506/233503.
(12) Kymakis, E.; Amaratunga, G. A. J. *Appl. Phys. Lett.* **2002**, *80*, 112−114.
(13) Rahman, G. M. A.; Guldi, D. M.; Cagnoli, R.; Mucci, A.; Schenetti, L.; Vaccari, L.; Prato, M. *J. Am. Chem. Soc.* **2005**, *127*, 10051−10057.
(14) Hirsch, A. *Angew. Chem., Int. Ed.* **2002**, *41*, 1853−1859.
(15) Tasis, D.; Tagmatarchis, N.; Bianco, A.; Prato, M. *Chem. Rev.* **2006**, *106*, 1105−1136.
(16) Banerjee, S.; Kahn, M. G. C.; Wong, S. S. *Chem.—Eur. J.* **2003**, *9*, 1898−1908.

Scheme 1. Pictorial Illustration of the *Top-Down* Approach to Obtain Molecules from SWNTs

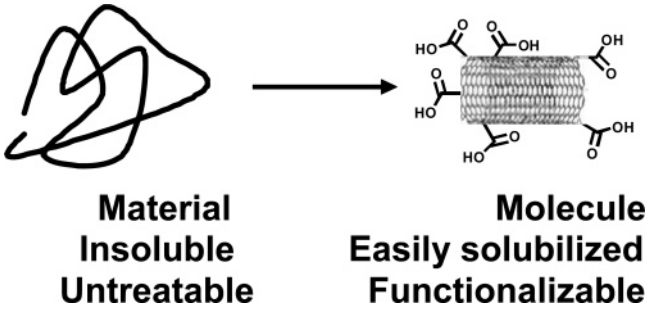

Among the drawbacks of as-synthesized SWNTs, the long aspect ratio (>10000) with tubes of micrometric length and nanometric diameter makes the material highly inappropriate to become dissolved in most solvents. In addition, the morphology of the nanotubes causes them to exhibit a large tendency to agglomerate forming bundles due to van der Waals forces.[17−19] In this regard, it will be of interest to have sufficiently short SWNTs with lengths below 500 nm in such a way that, on one hand, the units could be more easily solubilized and, on the other, debundling could render individual species of ideal dimensions entering in the molecular realm. In other words, cutting of SWNTs into short pieces followed by subsequent functionalization will produce compounds that could be envisioned more as truly molecular entities than as materials with infinite graphene tubes (Scheme 1). The properties of this novel class of molecules derived from SWNTs could be in many respects more alike to those of fullerene derivatives but with some remarkable differences such as the tubular geometry of the molecules with open tips and accessible hollow interior and a lower electron acceptor ability of the SWNT as compared to fullerenes among others distinctive features.

Aimed at preparing functional molecules from raw SWNTs, in this manuscript we report the covalent functionalization of short SWNTs (s-SWNTs) with strong electron acceptor photosensitizer pyrylium moieties and the observation of a photoinduced solubility increase of the resulting compound. This photoinduced solubility derives most probably from debundling of the pyrylium functionalized s-SWNT's as a consequence of photoinduced charge separation. Our system represents a case of *top-down* methodology in which starting from a insoluble solid material we have reduced over 2 orders of magnitude their length dimensions moving toward the preparation of individual molecular entities with photoresponsive solubility. To understand the properties of our compound, we will provide photophysical evidence that the pyrylium in its singlet and triplet electronic excited state acts as a strong electron acceptor termini and is able to interact with the s-SWNT residue. Pyrylium ions are well-known electron-transfer photosensitizers applicable for a wide range of substrates.[20] Photoinduced electron transfer is the elementary phenomenon responsible for the extensive debundling of the tubes that ultimately is reflected in a solubility increase.

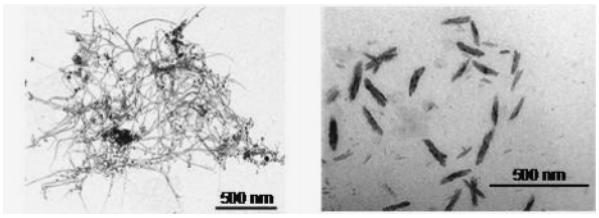

Figure 1. TEM images of the raw HiPCO SWNT used in this work (left) and the resulting s-SWNT obtained therefrom after harsh oxidative treatment (right). The dark spots in the raw HiPCO SWNT are due to the rest of the metallic catalyst and/or amorphous carbon.

Results and Discussion

Preparation and Characterization of Py-sSWNT. With the long-term goal of developing molecules from SWNTs, we proceeded to effect the purification of raw HiPCO SWNTs using a 3:1 mixture of concentrated H_2SO_4/HNO_3 acids at 40 °C for 24 h. It is well-known that oxidative acid treatment not only removes the rest of the metallic catalysts present in raw HiPCO SWNTs but also shortens the nanotube length by oxidatively cutting the nanotube at defects of the graphene layer with formation of carboxylic acid terminated tips.[21−22] It has been reported in the literature several studies correlating the severity and conditions of the oxidative acid treatment of SWNTs with the average length of the resulting material.[22−23] According to these studies we optimized our process in order to produce short SWNTs (s-SWNTs). Figure 1 presents selected images showing the initial SWNT and the resulting material after the acid oxidative treatment. As it can be seen in this figure, our oxidative treatment produces a remarkable effect in the aspect ratio of the raw HiPCO SWNT, with the obtainment of SWNT bundles below 200 nm in length (s-SWNT). Importantly, s-SWNT can be suspended uniformly in acetonitrile and other organic solvents, but it settles down upon standing for a few hours.

s-SWNT was functionalized through the carboxylic acid groups located mainly at the nanotube tips[14,24] with triarylpyrylium units as shown in Scheme 2. After reacting the carboxylic groups with sulfuryl chloride, the next step consisted in the formation of peptide bonds by reaction with 3-mercaptopropanamine. Afterward, the key step in the synthesis was the radical chain addition of mercapto groups to styryl C═C double bonds of a suitable 2,4,6-triarylpyrylium derivative. This reaction connecting the s-SWNT and the organic photo responsive subunit using catalytic amounts of azobis(isobutyronitrile) (AIBN) in oxygen-free toluene suspensions was essentially quantitative under very mild conditions (absence of acid or bases, oxidizing or reducing reagents), thus, being compatible with the presence of the pyrylium heterocycle.[25] Electrophilic addition of mercapto groups to styryl derivatives has been widely used in surface functionalization to obtain mesoporous silicas having covalently anchored organic moieties due to the high

(17) Dyke, C. A.; Tour, J. M. *J. Phys. Chem. A* **2004**, *108*, 11151−11159.
(18) Kim, O.-K.; Je, J.; Baldwin, J. W.; Kooi, S.; Pehrsson, P. E.; Buckley, L. J. *J. Am. Chem. Soc.* **2003**, *125*, 4426−4427.
(19) Star, A.; Liu, Y.; Grant, K.; Ridvan, L.; Stoddart, J. F.; Steuerman, D. W.; Diehl, M. R.; Boukai, A.; Heath, J. R. *Macromolecules* **2003**, *36*, 553−560.
(20) Galindo, F.; Miranda, M. A. *J. Photochem. Photobiol., A* **1998**, *113*, 155−161.
(21) Ziegler, K. J.; Gu, Z.; Peng, H.; Flor, E. L.; Hauge, R. H.; Smalley, R. E. *J. Am. Chem. Soc.* **2005**, *127*, 1541−1547.
(22) Liu, J.; Rinzler, A. G.; Dai, H.; Hafner, J. H.; Bradley, R. K.; Boul, P. J.; Lu, A.; Iverson, T.; Shelimov, K.; Huffman, C. B.; Rodriguez-Macias, F.; Shon, Y.-S.; Lee, T. R.; Colbert, D. T.; Smalley, R. E. *Science* **1998**, *280*, 1253−1256.
(23) Ziegler, K. J.; Gu, Z.; Shaver, J.; Chen, Z.; Flor, E. L.; Schmidt, D. J.; Chan, C.; Hauge, R. H.; Smalley, R. E. *Nanotechnology* **2005**, *16*, S539−S544.
(24) Alvaro, M.; Atienzar, P.; De la Cruz, P.; Delgado, J. L.; Troiani, V.; Garcia, H.; Langa, F.; Palkar, A.; Echegoyen, L. *J. Am. Chem. Soc.* **2006**, *128*, 6626−6635.
(25) Corma, A.; Garcia, H. *Adv. Synth. Catal.* **2006**, *348*, 1391−1412.

Scheme 2. Synthetic Routes Followed for the Preparation of s-SWNT, Py-SC_{12}, and Py-sSWNT

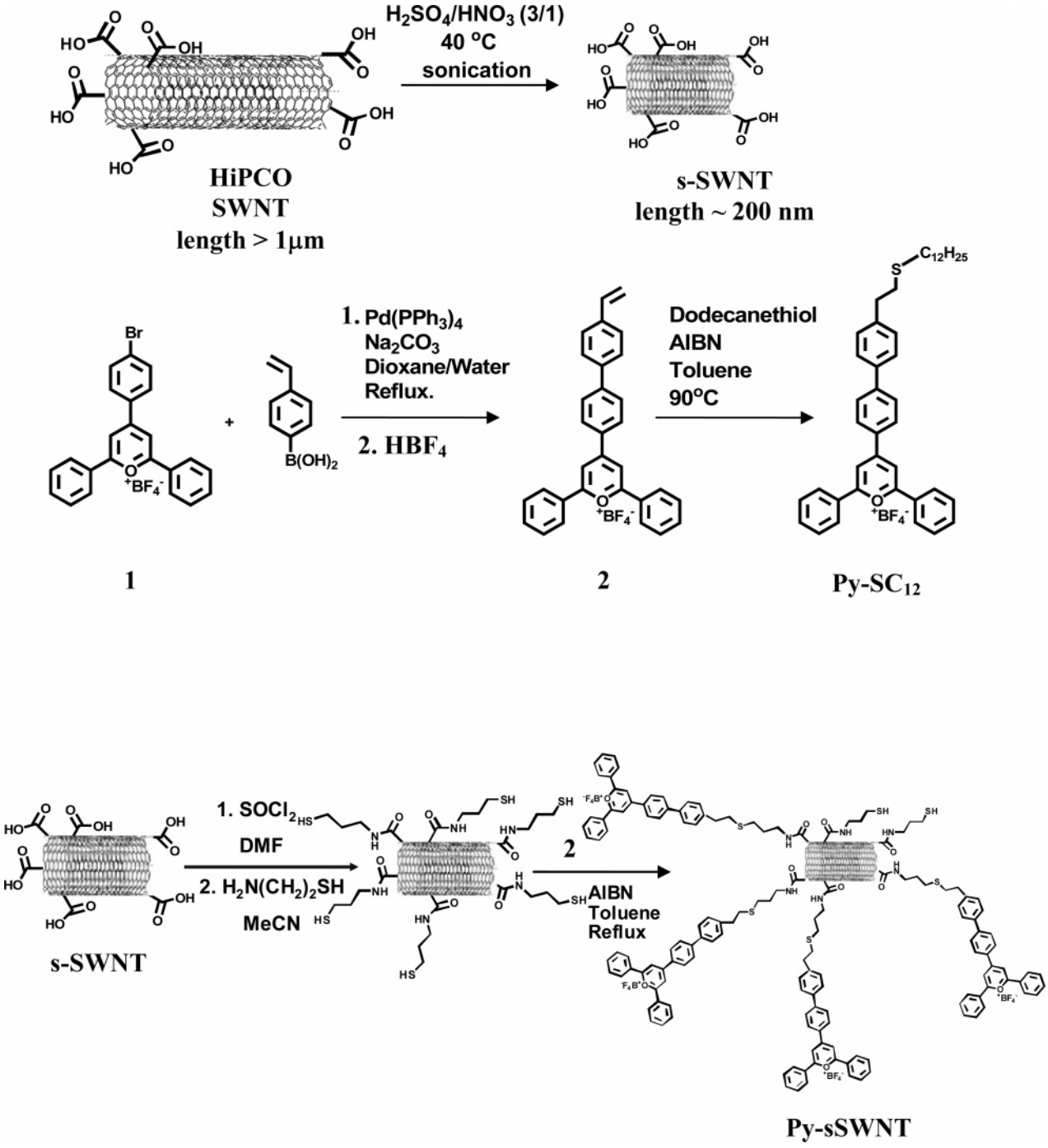

yield and selectivity of this reaction. Examples of quantitative thiol addition include the covalent anchoring of metal salen complexes[26,27] and carbapalladacycle catalysts to functionalized silicas.[28] As a control, a pyrylium derivative containing a thioether alkyl chain (Py-SC_{12}) was analogously prepared in essentially quantitative yields by AIBN initiated electrophilic addition of 1-dodecanethiol to the styryl derivative of 2,4,6-triarylpyrylium. Py-SC12 has the pyrylium heterocycle connected to a very similar structure as Py-sSWNT. The suitable 2,4,6-triarylpyrylium derivative having a styryl group was independently obtained by palladium-catalyzed Suzuki−Miyaura coupling[29,30] of 4-(4-bromophenyl)-2,6-diphenylpyrylium tetrafluoroborate and 4-vinylphenylboronic acid. Worth noting is the fact that after the C−C coupling the heterocyclic pyrylium core underwent ring opening, an additional acid treatment being necessary to reform the heterocyclic ring. This pyrylium ring opening is most probably due to the basic conditions required to effect the Suzuki coupling and the sensitivity of pyrylium ions to undergo hydrolytic ring opening under basic conditions.[31]

(26) Baleizao, C.; Gigante, B.; Das, D.; Alvaro, M.; Garcia, H.; Corma, A. *Chem. Commun.* **2003**, 1860−1861.
(27) Baleizao, C.; Gigante, B.; Garcia, H.; Corma, A. *J. Catal.* **2003**, *215*, 199−207.
(28) Corma, A.; Das, D.; Garcia, H.; Leyva, A. *J. Catal.* **2005**, *229*, 322−331.
(29) Heck, R. F. *Palladium Reagents in Organic Syntheses*; Academic Press: London, 1985.
(30) Tsuji, J. *Palladium Reagents and Catalysts: Innovations in Organic Synthesis*; Wiley: New York, 1995.

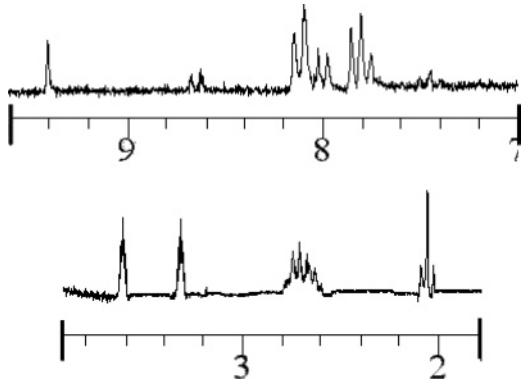

Figure 2. Relevant regions of ^{1}H NMR of purified Py-sSWNT in DMSO.

The sample of Py-sSWNT was dialyzed using a 2 kDa membrane to remove small weight impurities from the functionalized Py-sSWNT. A blank control in which a mixture of s-SWNT and $PySC_{12}$ (3.5 wt %) was dialyzed in water did not show the presence of $PySC_{12}$ in the resulting dialyzed solution, showing the performance of the membrane to effect purification of Py-sSWNT from small impurities.

The resulting Py-sSWNT was characterized by chemical analysis and spectroscopy. The maximum percentage of pyrylium functionalization was estimated by elemental combustion chemical analyses of N and S, giving a value of about 3.5 wt % of Py content in the material. The high-resolution 400 MHz ^{1}H NMR spectra of Py-sSWNT suspensions were recorded in DMSO and clearly show in the aromatic region the signals corresponding to the Py moiety. The protons corresponding to the mercaptopropyl amine linkers were also clearly distinguished in the aliphatic region. Figure 2 shows expansions proving the presence of the amido tethers and aromatic moieties on the ^{1}H NMR spectrum of Py-sSWNT. The δ values of the ^{1}H NMR firmly prove the covalent anchoring of the Py subunit on the s-SWNT. Thus, the signal at 3.6 ppm corresponds to the methylene next to the amide group, and it would have appeared at higher field if the linker was not bonded but a free amine. Also, no observation of the vinylic protons of compound **2** combined with the presence of the signals of two CH_2 groups bonded to S at 2.7 ppm is indicative that covalent anchoring has taken place.

The most characteristic feature in the UV−vis−NIR spectrum of s-SWNT is the absence of the van Hove absorption bands in the NIR. This fact is most probably a consequence of the short length of s-SWNT that can no longer be considered as an infinite graphene tube.[16,32] In addition, in the case of Py-sSWNT the presence of the Py chromophore is reflected in an increase in the absorbance at about 400 nm in the optical spectrum.

An interesting property that will become relevant when discussing the possibility of photoinduced electron transfer is the electrochemistry of Py-sSWNT and the two related model $Py\text{-}SC_{12}$ and s-SWNT compounds. As expected in view of the reported electrochemical studies on SWNTs in which no peaks are observed,[33−35] in our hands the cyclic voltammetry of Py-sSWNT or s-SWNT in deaerated dichloromethane did not allow detectable peaks attributable to electrochemical oxidation or reduction to be observed. Only resistive and capacitative currents were observed. Most probably the electrochemical responses of Py-sSWNT and s-SWNT are dominated by their relatively high electric conductivity that makes these compounds behave more like conductors than redox active molecules. In this case, the lack of response does not necessarily imply that Py-sSWNT and s-SWNT cannot donate or accept electrons but that, in the time scale of the electrochemical measurement (minutes), the charge from a working electrode cannot accumulate on these species.

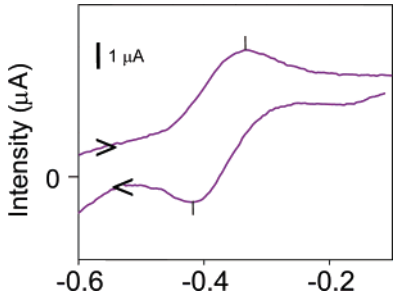

Figure 3. Cyclic voltammogram corresponding to $Py\text{-}SC_{12}$ in acetonitrile solution using 0.1 M of Bu_4N^+ ClO_4^- as electrolyte. Scan rate 50 $mV \cdot min^{-1}$.

In contrast to the SWNTs but in agreement with the electrochemical behavior of pyrylium ions,[36−38] $Py\text{-}SC_{12}$ exhibits in cyclic voltammetry a clear reversible, one-electron reduction peak at −0.38 V vs SCE (Figure 3). This reduction value is similar to those measured for the parent 2,4,6-triphenylpyrylium and other derivatives[36] and indicates that substitution on the heterocycle periphery does not alter much the electron acceptor ability of the core.

Upon anodic scan, no oxidation peak was observed at the maximum voltage available in our electrochemical study (+2 V), indicating that the sulfur atom of $Py\text{-}SC_{12}$ cannot be easily oxidized. In other words, an electron hole on the sulfur atom of the alkylthio chain must still be a strongly oxidizing site, with an oxidizing potential above +2 V. This point will become relevant when discussing the role of the sulfur atom as an electron hole relay in the photoinduced electron transfer (see below the discussion dealing with the laser flash photolysis of Py-sSWNT).

Taken together all the previous data are consistent with the covalent functionalization of s-SWNT with Py units. The presence of these pyrylium moieties and amide tethers are clearly revealed by the characteristic peaks in ^{1}H NMR spectroscopy. The short length of the s-SWNT scaffold and its Py-sSWNT derivative is clearly shown by TEM and is compatible with the disappearance of the van Hove absorptions in the NIR region. No evidence for any complexation in the ground state between the Py and the nanotube moieties was obtained, although the low Py content makes this issue difficult to assess at this point.

(31) Graphakos, B. J.; Katritzky, A. R.; Lhommet, G.; Reynold, K. *J. Chem. Soc., Perkin Trans.* **1980**, *1*, 1345−1346.
(32) Umek, P.; Seo, J. W.; Hernadi, K.; Mrzel, A.; Pechy, P.; Mihailovic, D. D.; Forro, L. *Chem. Mater.* **2003**, *15*, 4751−4755.
(33) Ehli, C.; Rahman, G. M. A.; Jux, N.; Balbinot, D.; Guldi, D. M.; Paolucci, F.; Marcaccio, M.; Paolucci, D.; Melle-Franco, M.; Zerbetto, F.; Campidelli, S.; Prato, M. *J. Am. Chem. Soc.* **2006**, *128*, 11222−11231.
(34) Day, T. M.; Wilson, N. R.; Macpherson, J. V. *J. Am. Chem. Soc.* **2004**, *126*, 16724−16725.
(35) Stoll, M.; Rafailov, P. M.; Frenzel, W.; Thomsen, C. *Chem. Phys. Lett.* **2003**, *375*, 625−631.
(36) Domenech, A.; Domenech-Carbo, M. T.; Garcia, H.; Galletero, M. S. *Chem. Commun.* **1999**, 2173−2174.
(37) Domenech, A.; Garcia, H.; Domenech-Carbo, M. T.; Galletero, M. S. *Anal. Chem.* **2002**, *74*, 562−569.
(38) Miranda, M. A.; Garcia, H. *Chem. Rev.* **1994**, *94*, 1063−1089.

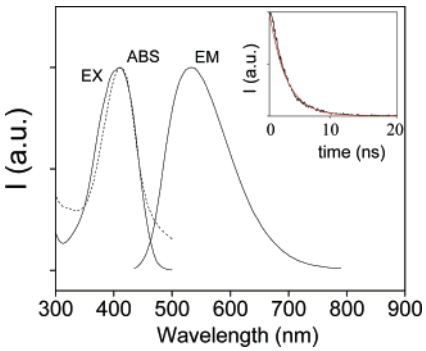

Figure 4. Emission (EM, $\lambda_{exc} = 412$ nm), excitation (EX, $\lambda_{em} = 533$ nm), and absorption (ABS) spectra of a deareated acetonitrile solution of the sample Py-SC_{12}. The inset shows the temporal profile of the signal monitored at 533 nm and the best fitting (continuous line) to a single monoexponential decay.

Emission Studies: Proof of the Interaction between the Pyrylium and SWNT Moieties in Py-sSWNT. Convincing evidence of the interaction between Py and s-SWNT can be obtained by observing the changes in the photophysical properties of Py-SC_{12} upon increasing concentrations of s-SWNT. As most pyrylium ions, Py-SC_{12} emits fluorescence (λ_{fl} 533 nm) upon excitation at absorption λ_{max} (412 nm). The quantum yield of this emission (Φ 0.14) is about one-half that of the parent 2,4,6-triphenylpyrylium (Φ 0.33) and may reflect the effect of the S atom on the emission intensity (see below for S quenching). Figure 4 shows the fluorescence and the excitation spectra, including a comparison with the absorption spectrum. The good match between the excitation and the absorption spectra indicates that the emission originated from excitation of the Py-SC_{12} ground state. The fluorescence temporal profile fits relatively well to the single-exponential decay with a half-life of 2.4 ns (inset of Figure 4). The $E_{0,0}$ energy of the singlet excited state can be estimated as 61 kcal·mol^{-1} from the interception between the ground UV−vis absorption and fluorescence spectra. Then, by applying the Rehm−Weller formalism,[39] it can be deduced that the oxidation potential of the Py-SC_{12} singlet excited state is higher than 2.5 V.

Addition of s-SWNT quenches the emission of Py-SC_{12}. The estimated Stern−Volmer quenching constant was obtained plotting the relative I_o/I fluorescence intensity measured at the emission wavelength maximum vs the amount of s-SWNT added to the solution in mg·L^{-1}. Considering a fluorescence τ_o of 2.4 ns (estimated from single photon counting), this gives an equivalent quenching rate constant of 9.1×10^9 s^{-1}·mg^{-1}·L for s-SWNT.

Also the reverse situation, i.e., emission of s-SWNT quenched by Py-SC_{12}, was observed. s-SWNT shows a continuous absorption with onset at 800 nm; thus, it is possible to envision a situation in which the absorbing chromophore is the nanotube rather than the Py unit. For this reason, it is of interest to determine if, upon excitation of the carbon nanotube moiety, there are specific properties of Py-sSWNT arising from the interaction between the two subunits. Like an SWNT of micrometric length,[40,41] s-SWNT exhibits weak emission (λ_{em} 330 nm) upon excitation at short wavelengths (λ_{ex} 280 nm). The quantum yield of emission was 0.09. This emission also decreases in intensity upon addition of Py-SC_{12}. Quantitative measurements are, however, not possible in this case due to the fact that Py-SC_{12} as a quencher also absorbs at the excitation wavelength used to monitor the s-SWNT emission.

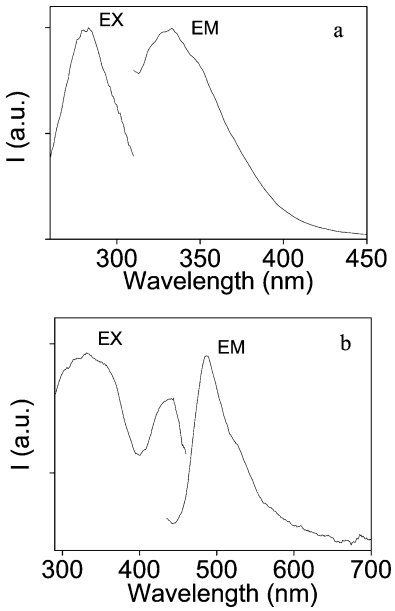

Figure 5. Emission spectra (EM) of Py-sSWNT upon excitation at the s-SWNT subunit (280 nm, a) and pyrylium moiety (415 nm, b). The corresponding excitation spectra (EX) have been obtained upon monitoring at the corresponding λ_{fl}.

Fluorescence studies as a tool to show the interaction in the excited electronic states between the pyrylium and the nanotube subunits were completed by determining the emission of Py-sSWNT in which the two moieties are covalently linked. Comparison of the emission properties of Py-sSWNT with those of the two subunits independently also provides useful information, particularly about the importance of having a covalent tether connecting the components with respect to their mixture. In this context, Py-sSWNT exhibits two distinctive emission spectra depending on the excitation wavelength. The characteristic features of these two emissions in terms of λ_{ex} and λ_{em} can be easily interpreted as arising from the independent emission of each of the two chromophores either Py or s-SWNT. Figure 5 shows the spectra corresponding to the variation of λ_{em} as a function of λ_{ex}. Interestingly, Φ of these two emissions (<0.01) is significantly smaller than those of Py-SC_{12} and s-SWNT considered as model compounds and smaller than a mixture of Py-SC_{12} and s-SWNT in the proportion equivalent to Py-sSWNT. These observations indicate that the interaction between the two subunits experience a synergy as a consequence of the covalent tethering with respect to a mixture of their individual components.

Laser Flash Photolysis Py-SC_{12} and s-SWNT Model Compounds. The photochemistry of 2,4,6-triarylpyrylium ions has attracted considerable attention due to the wide use of these heterocycles as electron-transfer photosensitizers.[20,38,42] It is known that the singlet excited state undergoes an efficient intersystem crossing with formation of the corresponding triplet excited state that has a lifetime of a few microseconds.[38] Both

(39) Gilbert, A.; Baggott, J. *Essentials of Organic Photochemisry*; Blackwell: Oxford, 1990.
(40) Alvaro, M.; Atienzar, P.; Bourdelande, J. L.; Garcia, H. *Chem. Commun.* **2002**, 3004−3005.
(41) Alvaro, M.; Atienzar, P.; de la Cruz, P.; Delgado, J. L.; Garcia, H.; Langa, F. *Chem. Phys. Lett.* **2004**, *386*, 342−345.
(42) Kavarnos, G. J.; Turro, N. J. *Chem. Rev.* **1986**, *86*, 401−449.

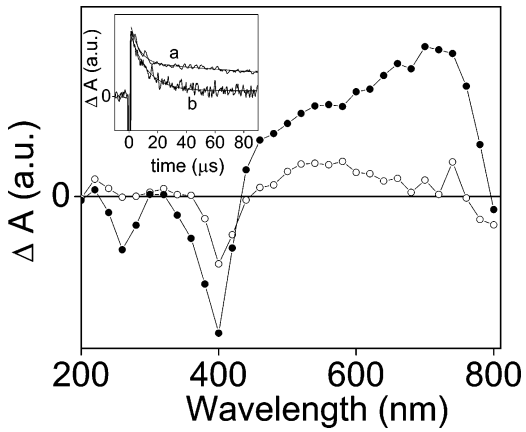

Figure 6. Transient absorption spectra of an acetonitrile solution of Py-SC_{12} (4×10^{-5} M) recorded 2 (●) and 81 (○) μs after 355 nm laser excitation under N_2 atmosphere. The inset shows the decay of the signal monitored at 550 (a) and 700 (b) nm.

singlet and triplet excited states can be quenched by electron donors giving rise to the formation of the corresponding pyrylium radical that has a lifetime of hundreds of microseconds.

The photochemistry of Py-SC_{12} as a model compound for Py-sSWNT follows this expected general pattern. Thus, upon 355 nm laser excitation of a deaerated acetonitrile solution of Py-SC_{12}, an intense transient spectrum was recorded. No permanent product formation was observed, and the optical spectrum and absorbance value of the Py-SC_{12} remained unaltered after the laser flash photolysis experiments. The transient spectrum shows bleaching of Py-SC_{12} ground state absorption at λ_{max} 250 and 400 nm together with an absorption band from 415 to 800 nm. The spectrum changes over time indicating that this band corresponds to more than one species. Figure 6 shows selected transient spectra recorded at different delay times after the laser pulse to illustrate these spectral variations as well as the temporal profile of the signal measured at 550 and 700 nm. Oxygen purging quenches the absorption at λ_{max} 750 nm, and therefore, absorption in the 600−800 nm was assigned to the T−T absorption of the Py-SC_{12} triplet excited state. The decay of the signal monitored at 700 nm fits monoexponential kinetics with a half-life of 11.7 μs. The reported triplet excited state of related 2,6-diphenyl-4-biphenylpyrylium tetrafluoroborate shows similar spectroscopic and lifetime features ($\lambda_T = 700$ nm; $\tau_T = 5$ μs).[43]

At longer elapsed times after the laser flash or in the presence of oxygen, a residual ground state bleaching and an absorption band at λ_{max} 525 nm was recorded. Based on the similarity with the optical spectrum of analogous pyrylium radicals,[38] this transient spectrum was assigned to the Py-SC_{12} radical arising from the electron-transfer quenching of the pyrylium electronic excited states by the sulfur atoms as electron donors. The recovery of the ground state measured at 400 nm and the decay of the signal monitored at 525 nm were coincident and could be fitted to a monoexponential kinetics with a half-life of 147 μs. Thus, annihilation by back electron transfer is the deactivation pathway for this charge-separated species. The fact that the transient signal of the radical recorded at 525 nm does not show a growth in the time scale in which triplet is decaying rules out that the charge-separated state originated from the triplet and, therefore, should be exclusively generated from the Py-SC_{12} singlet excited state. The relative quantum yield for triplet formation and photoinduced electron transfer was estimated to be approximately equal based on the ground state bleaching of Py-SC_{12} at 400 nm measured at 10 (triplet plus charge separated states) and 100 μs (charge separate state). The molar absorptivity of the triplet excited band at 720 nm and the $Py^{\bullet}$-$S^{+\bullet}C_{12}$ radical at 525 nm was 36 190 and 16 402 $mol^{-1}\cdot L\cdot cm^{-1}$, respectively. Scheme 3 summarizes the photochemistry and the main kinetic data determined for Py-SC_{12}.

Scheme 3. Main Photophysical Data Measured for Py-SC_{12}

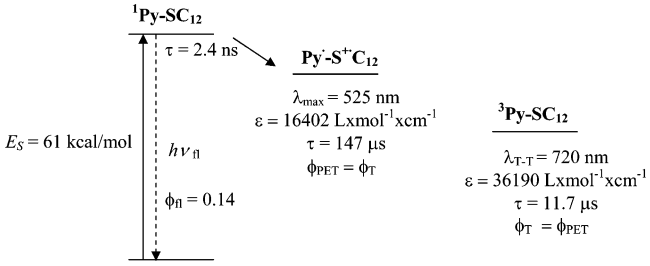

Concerning the structure of the Py-SC_{12} radical arising from the photoinduced intra- or intermolecular electron transfer, the electron gained by the pyrylium acceptor core is most probably donated by the sulfur atom. Then, a radical cation center will be created in this heteroatom. In this context it is worth commenting whether the presence of a S atom in the tether plays a positive or a negative role on the interaction of the pyrylium subunit with the s-SWNT moiety. As mentioned earlier when presenting the cyclic voltammetry studies of Py-SC_{12} and, more specifically, from the lack of oxidation peak, it is inferred that the positive hole at the S atom should have an oxidation potential above +2 V and, therefore, is strongly oxidizing. Therefore, the oxidation potential of the Py-SC_{12} radical should be in the interval between the oxidation potential of the singlet excited state (>2.5 V vs SCE) and +2 V vs SCE that is the maximum of the electrochemical potential. Actually, the energy of the charge separated state must also be above that of the triplet excited state, since $Py^{\bullet -}-SC_{12}^{\bullet +}$ is not generated by triplets. Thus, from the thermodynamic point of view the presence of a S atom should reduce somewhat the driving force for oxidation of the carbon nanotube. However, from the kinetic point of view, the presence of a sulfur atom plays a positive role intercepting the short-lived singlet excited state (τ 2.4 ns) and producing with significant efficiency much longer lived radicals (τ 147 μs) that still are strongly oxidant. Thus, in a certain way, the sulfur atom of the tether is acting as an electron hole relay spanning the lifetime of charge separation by about 10^5 times and facilitating the kinetics of the photoinduced electron transfer from the best electron donor site of the molecule to the final pyrylium terminus.

In contrast to Py-SC_{12}, s-SWNT shows upon laser flash photolysis a weak transient absorption spectrum that consists on a very broad, structureless band spanning the whole wavelength range (200−800 nm). Only a minor absorbance increase (from 0.30 to 0.35 OD units at 250 nm) was observed in the UV region of the optical spectrum of the photolyzed s-SWNT acetonitrile suspension after the laser flash photolysis study. This variation in the optical spectrum of s-SWNT upon photolysis was interpreted as reflecting an increase in the debundling of the sample. Nevertheless, the time-resolved

(43) Alvaro, M.; Aprile, C.; Carbonell, E.; Ferrer, B.; Garcia, H. *Eur. J. Org. Chem.* **2006**, 2644−2648.

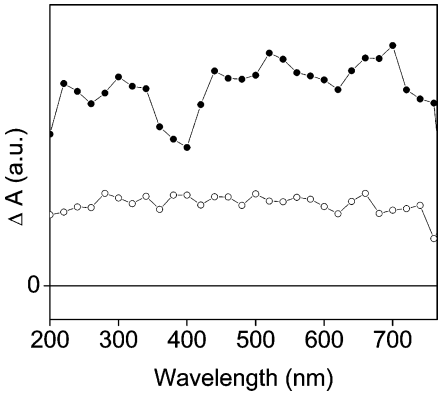

Figure 7. Transient absorption spectra of s-SWNT (○) and of a mixture of Py-SC_{12} and s-SWNT in a proportion equivalent to that of Py-sSWNT (●) in deaerated acetonitrile recorded 2 μs after 355 nm laser excitation.

spectrum of the s-SWNT suspension was also recorded under dynamic flow, but this spectrum was coincident to that recorded for a suspension in a quartz cuvette. Figure 7 shows the transient spectrum recorded 2 μs after 355 nm excitation of a deaerated s-SWNT acetonitrile suspension. The temporal profiles of the signal monitored at different wavelengths were coincident suggesting that the spectrum corresponds to a single transient species.

When a mixture of Py-SC_{12} and s-SWNT in a proportion equivalent to that of Py-sSWNT (3,5 wt % in Py) was submitted to 355 nm laser flash in deareated acetonitrile, the resulting spectrum showed absorption bands attributable to the Py-SC_{12} triplet (750 nm) and Py$^{\bullet}$-SC_{12} radical (525 nm), together with an absorption from 200 to 400 nm that was not previously detected for any of the model molecules. Figure 7 also contains the spectrum recorded for the Py-SC_{12}/s-SWNT mixture suspended in deaerated acetonitrile compared to that of s-SWNT. Given the strong electron acceptor ability of Py-SC_{12} in its excited state, the absorption appearing in the 200−400 nm can be attributed to the generation of positive electron holes on the s-SWNT. The fact that the pyrylium radical (525 nm band) is formed by electron abstraction exclusively from the S atoms as in the case of pure Py-SC_{12} would not explain the presence of the intense 200−400 nm band, previously not observed for either Py-SC_{12} or s-SWNT. In agreement with our proposal, the 200−400 nm broad band and the 525 nm were not quenched by oxygen.

Laser Flash Photolysis of Py-sSWNT. As it could be anticipated in view of the data obtained for the model molecules, the laser flash photolysis spectrum of Py-sSWNT consisted of a broad absorption from 200 to 500 nm, peaking at 280 nm, together with a weak band at 550 nm. Figure 8 shows the transient spectrum recorded 1.2 μs after the 355 nm laser flash. The temporal profiles of the 280 and 550 nm bands were significantly different. They were fitted to monoexponential kinetics with half-lives of 6.4 and 1.5 μs for the 280 and 550 nm bands, respectively. These two features, but particularly the presence of the broad 200−500 nm band, are compatible with the occurrence of a photoinduced electron transfer from the s-SWNT to the Py unit of the Py-sSWNT to give an electron hole on s-SWNT (absorption band at λ_{max} 280 nm) and the Py radical (λ_{max} 550 nm). The poor resolution of the transient spectrum due to the colloidal nature of the samples precluded detailed quantitative quenching studies, but in accordance with

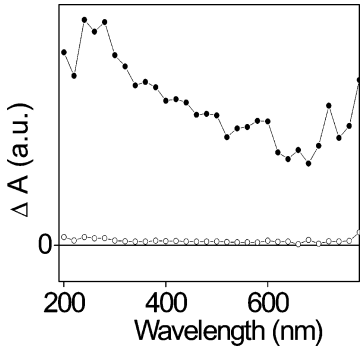

Figure 8. Transient absorption spectrum of Py-sSWNT in deaerated acetonitrile recorded 1.2 (●) and 8 (○) μs after 355 nm laser excitation.

our proposal the presence of methanol (hole quencher) quenched the band at 280 nm, but not the 550 nm peak. The possibility that the sulfur atom of the linker is exclusively the electron donor seems unreasonable in view of the presence of the 200−500 nm absorption that is exclusively due to the nanotube moiety.

Fullerenes are extremely good electron acceptors, and they can rarely be oxidized.[44] This strong electron acceptor ability of fullerenes derives from the spherical geometry and strong distortion of the sp^2 orbitals. Cyclic voltammetry of fullerene reveals up to six reduction peaks and no anodic oxidation.[45,46] The electrochemistry of SWNTs is totally different from that of fullerenes. SWNTs are more versatile, since it has been reported that they can accept and donate electrons depending on the redox potential of the partner. Particularly related to our work is the behavior of SWNTs functionalized with viologens.[47] Viologens are among the strongest electron acceptors, and they have a long-lived, blue radical cation that can be easily detected by steady-state and transient spectroscopy due to their intense and characteristic absorption bands.[48] For the viologen-functionalized SWNT, detection of the viologen radical cation was presented as evidence of photoinduced electron transfer from the SWNT to viologen.[47]

Photosolubility of Py-sSWNT. As commented on in the introduction, one general problem associated to SWNTs is their tendency to agglomerate forming bundles. Agglomeration arises from weak van der Waals forces between the walls of the nanotubes and is a phenomenon that negatively affects many SWNT properties, which will benefit the existence of individual nanotubes. Solubility is one of these properties that ideally would require debundling. Several strategies including the use of surfactants and covalent/noncovalent functionalization have been reported to produce the deagglomeration of SWNTs.[49]

In the case of Py-sSWNT, upon illumination of a stirred suspension in aqueous or organic solvent, a remarkable increase in the solubility of the molecule occurred. This solubility increase can be visually followed by the increase in the solution

(44) Giacalone, F.; Segura, J. L.; Martin, N.; Ramey, J.; Guldi, D. M. *Chem.—Eur. J.* **2005**, *11*, 4819−4834.
(45) Xie, Q.; Perez-Coredero, E.; Echegoyen, L. *J. Am. Chem. Soc.* **1992**, *114*, 3978−3980.
(46) Sun, N.; Guan, L.; Shi, Z.; Zhu, Z.; Li, N.; Li, M.; Gu, Z. *Electrochem. Commun.* **2005**, *7*, 1148−1152.
(47) Alvaro, M.; Aprile, C.; Atienzar, P.; Garcia, H. *J. Phys. Chem. B* **2005**, *109*, 7692−7697.
(48) Monk, J. A. *The Viologens: Physicochemical Properties, Synthesis and Applications of Salts of 4,4′-Bipyridine*; Wiley: New York, 1998.
(49) Yerushalmi-Rozen, R. In *PCT Int. Appl.* (Ben-Gurion University of the Negev Research and Development Authority, Israel). Wo, 2005, p 26 pp.

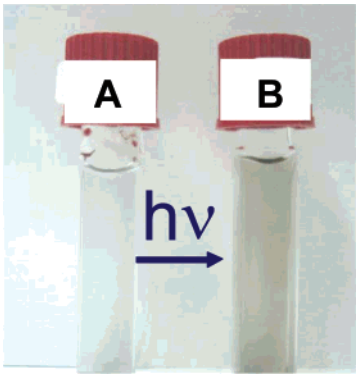

Figure 9. Photographs illustrating the changes in the appearance of an acetonitrile solution of the Py-sSWNT induced by illumination.

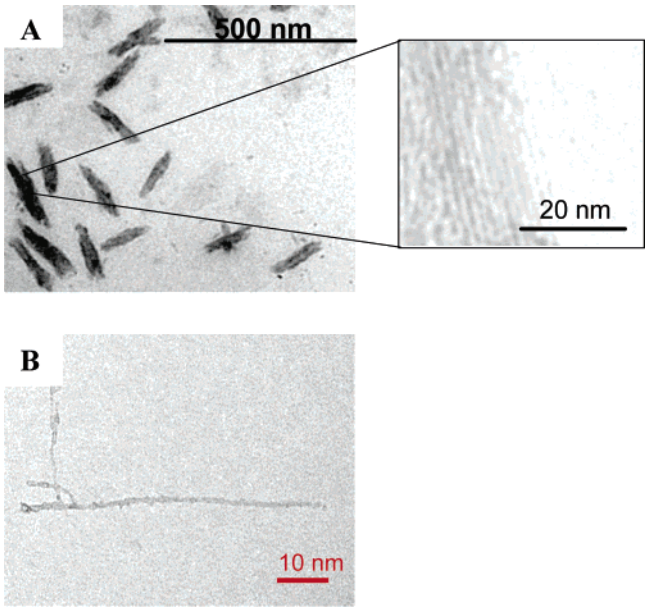

Figure 10. TEM images of an acetonitrile solution of the sample Py-sSWNT before (a) and after (b) laser irradiation showing the presence of agglomerated (a) and isolated (b) nanotubes.

color intensity. A quantitative estimation was performed monitoring the absorbance increase at 400 nm. Figure 9 shows two photographs illustrating the changes in the appearance of the solution induced by light. Upon extended illumination, up to 2 wt % of Py-sSWNT can be dissolved in water and acetonitrile. This value corresponds to a 1 order of magnitude higher concentration than that of the unirradiated sample kept in the dark. Comparison of TEM images before and after illumination shows that the solubility increase is due to photoinduced debundling of the Py-sSWNT. Figure 10 shows selected TEM images to illustrate the changes in the morphology of the material at the microscopic level upon illumination.

Based on the photophysical information obtained above, we propose that the photoinduced solubility increase is due to deagglomeration of the Py-sSWNT, individual molecules being more soluble than aggregates. This deagglomeration arises from the charge separation produced by photoinduced electron transfer from the sSWNT to the Py subunits, producing the positive charging of the nanotube walls. Coulombic repulsion between the positive nanotube walls will be the force responsible for

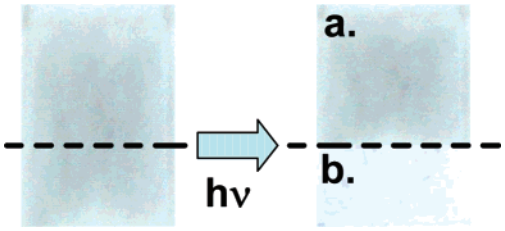

Figure 11. A film of Py-sSWNT cast on a glass slide before (left) and after (right) acetonitrile washings. The lower half (part b) was exposed to a laser beam (308 nm) for 15 min (pulse frequency 1 Hz) before solvent washings.

the deagregation and separation of the tubes into individual molecules by compensating the weak attractive van der Waals forces.

Photoinduced solubilization is a process of technological relevance that is the base of current photoresists for microchip production and patterning in general.[50,51] In fact, the above observation of photoresponsive solubilization can also serve for patterning carbon nanotube layers in which the material will be selectively solubilized in the illuminated regions. To demonstrate the feasibility to apply this photoinduced solubilization for patterning, we cast a film of Py-sSWNT on a glass slide and expose one-half to a laser beam (308 nm, 1 × 2.5 cm^2). After 15 min of laser exposure (repetition frequency 1 Hz, 20 $mJ \cdot pulse^{-1}$), the slide was thoroughly washed with acetonitrile, and while the unirradiated half resulted in being almost unchanged, a significant portion of the irradiated half was easily dissolved. Figure 11 shows some photographs to illustrate the applicability of photoinduced solubility for nanotube patterning.

Experimental Section

All the solids were analyzed by combustion chemical analysis performed in a FISONS CHNOS analyzer. FT-IR spectra were recorded with a Nicolet 710 FT-IR spectrophotometer. The IR spectra were recorded at room temperature under vacuum after outgassing the sample at 200 °C. High-resolution mass spectrometry was performed using a VG Autospec. The TEM images were obtained using a Philips CM300 FEG system with an operating voltage of 100 kV. ^1H and ^{13}C NMR spectra were recorded with $CDCl_3$ as solvent using TMS as internal standard in a Bruker Avance (300 MHz) spectrometer for compounds **1** and **2** and in a Bruker Avance (400 MHz) spectrometer for the Py-sSWNT.

Cyclic voltammetry was carried out using an Amel Instruments MOD.7050 potentiostat equipped with Amel-Junior AssisrV2 software. All the measurements were performed in acetonitrile in the presence of tetrabutylammonium perchlorate (0.1 M) and recorded between −2.0 and 2.0 V at a scan speed of 50 mV/s.

UV−vis absorption spectra were recorded with a Perkin-Elmer λ35 spectrophotometer. Fluorescence spectra and lifetimes were recorded on an Edinburgh Analytical Instruments FL900 spectrophotometer. Laser flash photolysis experiments were carried out in a Luzchem nanosecond laser flash system using the third (355 nm, 20 mJ/pulse) harmonic of a Surelite Nd:YAG laser for excitation (pulse ≤10 ns) and a 175 W ceramic Cermax Xenon Fiberoptic Light source, perpendicular to the laser beam, as a probing light. The signal from the monochromator/photomultiplier detection system was captured by a Tektronix TDS 3032B digitizer. The laser system and digitizer are

(50) Chen, X.; Rogach, A. L.; Talapin, D. V.; Fuchs, H.; Chi, L. *J. Am. Chem. Soc.* **2006**, *128*, 9592−9593.
(51) Chigrinov, V. G.; Kozenkov, V. M.; Kwok, H. S. *Opt. Appl. Liq. Cryst.* **2003**, 201−244.

connected to a PC computer via GPIB and serial interfaces that controlled all the experimental parameters and provided suitable processing and data storage capabilities. The software package has been developed in the LabVIEW environment from National Instruments and compiled as a stand-alone application. Fundamentals of similar time-resolved laser setups have been published elsewhere.[52] The samples contained on a suprasil quartz 0.7 cm × 0.7 cm cuvette capped with septa were purged with N_2 flow at least 15 min before laser experiments.

Synthesis of Compound 1. To a solution of 4-bromobenzaldehyde (1.54 g, 8.32 mmol) in dichloromethane (30 mL) were sequentially added acetophenone (2.00 g, 1.66 mmol) and $BF_3(Et)_2O$ (2.7 mL). The mixture was stirred for 24 h at reflux temperature and then cooled and treated with Et_2O (60 mL). The solvent was removed by filtration to give after drying the 4-(4-bromophenyl)-2,6-diphenylpyrilium tetrafluoroborate (**1**) as yellow powder (2.87 g, 76% yield). ^{1}H NMR ($CDCl_3$, 300 MHz) δ 7.85 (t, J = 7.4 Hz, 2H), 7.93 (d, J = 7.5 Hz, 1H), 8.00 (d, J = 9.0 Hz, 1H), 8.55 (d, J = 9 Hz, 1H), 8.69 (d, J = 7.4 Hz, 1H), 9.26 (s, 1H). ^{13}C NMR ($CDCl_3$, 75 MHz) δ 115.0, 128.6, 128.8, 129.5, 130.9, 132.6, 134.8, 164.4, 170.8. IR (liquid film) ν_{max} = 1484, 1592, 1623 cm^{-1}. Combustion chemical analysis: theoretical for $C_{23}H_{16}BrO_2 \cdot BF_4 4(H_2O)$ (%): C, 51.62; H, 4.52. Found (%): C, 49.80; H, 3.25.

Synthesis of Compound 2. 4-Vinylphenylboronic acid (0.47 g, 3.15 mmol) was dissolved in dioxane (5 mL), and tetrakis(triphenylphosphine)palladium catalyst (76 mg) was added. Then a 2 M solution of Na_2CO_3 (4.3 mL) and compound **1** (1.00 g, 2.1 mmol) were simultaneously added. The mixture was stirred at reflux temperature for 3 h and then cooled, and the catalyst was removed by filtration. The liquid was extracted with diethyl ether, and the organic layer was washed with a tetrafluoroboric acid solution (10^{-2} M), dried under $MgCO_3$, and evaporated under reduced pressure to give compound **2** as a red orange solid. ^{1}H NMR ($CDCl_3$, 300 MHz) δ 5.38 (d, J = 11.7 Hz, 1H), 5.98 (d, J = 17.4 Hz, 1H), 6.89 (dd, J = 11.7 and 17.4 Hz, 1H), 7.54−7.85 (m, H), 8.12 (d, J = 8.4 Hz, 1H), 8.72 (dd, J = 7.4 and 12.2 Hz, 2H), 9.3 (s, 1H). ^{13}C NMR ($CDCl_3$, 75 MHz) δ 14.5, 126.5, 126.9, 127.4, 128.2, 128.9, 129.5, 130.2, 134.6, 155.5, 172.4. IR (liquid film) ν_{max} = 1592, 1623, 1650, 1679, 2917, 3021, 3077 cm^{-1}.

Synthesis of Py-SC$_{12}$. To a solution of **2** (10 mg, 0.2 mmol) in deareated acetonitrile (5 mL) were sequentially added 1-dodecanethiol (80 mg, 0.40 mmol) and *a*,*a*′-azoisobutyronitrile (AIBN) in a catalytic amount. The mixture was stirred overnight at reflux temperature under nitrogen atmosphere. Then the solvent was removed under reduced pressure, and the solid was washed with methanol to give Py-SC$_{12}$ like a red-orange powder. ^{1}H NMR (CD_3OD, 300 MHz) δ 0.98 (t, J = 7.8 Hz, 3H), 1.27−1.39 (m, 4H), 1.82 (t, J = 7.84, 2H), 1.97−1.39 (m, 18H), 4.15 (t, J = 7.2, 2H), 7.84−7.94 (m, 6H, ArH), 8.47−8.59 (m, 4H, ArH), 9.02 (8s, 1H, ArH). ^{13}C NMR (CD_3OD, 75 MHz) δ 14.5, 126.5, 126.9, 127.4, 128.2, 128.9, 129.5, 130.2, 134.6, 155.5, 172.4. IR (liquid film) ν_{max} = 1492, 1592, 1623, 1850, 2923 cm^{-1}. HRMS: 613.3499 (M^+) calculated for $C_{13}H_{23}O^+$ 613.3504.

Cutting and Chlorination of HiPCO Single Wall Nanotube (SWNT). Raw HiPCO SWNT (500 mg) was suspended in 10 mL of a 3:1 mixture of sulfuric and nitric acid. The mixture was sonicated at 40 °C for 30 min, then neutralized with NaOH, and filtered under vacuum. The short SWNTs (s-SWNTs) were characterized by Raman and transmission electron microscopy.

Formation of the chlorinated SWNT was accomplished by suspending purified s-SWNTs (100 mg) in $SOCl_2$ (10 mL). The mixture was stirred at 65 °C for 24 h and then cooled at room temperature. The solid was allowed to settle down, and the $SOCl_2$ was cautiously removed. THF was added, and the mixture was filtered under vacuum and washed with additional THF.

Synthesis of s-SWNT and Py-sSWNT. The chlorinated s-SWNT (200 mg) was suspended in THF (5 mL), and K_2CO_3 (150 mg) and 3-ammoniumpropylthiol chloride (150 mg) were sequentially added. The mixture was stirred at reflux temperature for 20 h, then cooled at room temperature, and filtered. The solid was washed with THF and methanol to remove the excess reactants. Combustion chemical analysis of the black powder reveals that the s-SWNT was functionalized in 14 wt % (combustion chemical analyses found (%): C, 49.54; H, 1.96; N, 2.60; S, 5.36). This solid was directly used for the next step without ulterior purification.

The 3-mercaptopropylamido functionalized s-SWNT (100 mg) was suspended in acetonitrile, and compound **2** (90 mg, 0.19 mmol corresponding to 1 equiv with respect to the thiol functionalization of s-SWNT) and AIBN in a catalytic amount were added. The mixture was stirred overnight at reflux temperature, then filtered under vacuum, and washed with methanol. The resulting Py-s-SWNT was characterized by ^{1}H NMR and chemical analysis.

^{1}H NMR (DMSO, 700 MHz) δ 2.07 (t, J = 7.7 Hz, 2H), 2.61−2.80 (m, 2H), 3.25 (t, 2H), 3.62 (t, 2H), 7.53 (d, J = 7.2 Hz, 2H, ArH), 7.67 (t, J = 6.9 Hz, 4H, ArH), 8.02 (d, J = 9.2 Hz, 2H, ArH), 8.18 (d, J = 7.6 Hz, 4H, ArH), 8.63 (d, J = 6.7 Hz, 2H, ArH), 9.20 (s, 1H, ArH). Combustion chemical analysis found (%): C, 52.64; H, 1.99; N, 3.00; S, 5.10.

Acknowledgment. Dedicated to Prof. Miguel Yus on occasion of his 60th anniversary. Financial support by the Spanish DGI (Grants and CTQ06-06758) is gratefully acknowledged. C.A. and B.F. also thank the Spanish Ministry of Education for two research associate Juan de la Cierva contracts.

JA0690520

(52) Kelly, G.; Willsher, C. J.; Wilkinson, F.; Netto-Ferreira, J. C.; Olea, A.; Weir, D.; Johnston, L. J.; Scaiano, J. C. *Can. J. Chem.* **1990**, *68*, 812−819.